X-RAY AMORPHOUS SULFATES IN GALE CRATER. R. J. Smith[1], S. M. McLennan[1], C. N. Achilles[2], E. Dehouck[3], B. N. Horgan[4], N. Mangold[5], E. B. Rampe[6], M. Salvatore[7], K. Siebach[8], V. Sun[9], [1]Stony Brook University (rebecca.j.smith@stonybrook.edu), [2]NASA Goddard Space Flight Facility, [3]Université de Lyon, [4]Purdue University, [5]Univesité de Nantes, [6]NASA Johnson Space Center, [7]Northern Arizona University, [8]Rice University, [9]Jet Propulsion Laboratory.

Introduction: The Mars Science Laboratory (MSL) mission is approaching an important transition from rock units with clay mineral spectral signatures into rock units with sulfate spectral signatures, potentially marking a period of climate change in Mars' history [1]. In order to fully appreciate the nature and extent of this transition, it is important to understand the full range of sulfate phases present in Gale crater up to this point.

A range of sulfate mineral compositions has been observed along the rover traverse. Light-toned diagenetic features, such as veins are predominantly identified as Ca-sulfates by the ChemCam instrument [2-4], and the CheMin XRD instrument has identified mostly Ca-sulfates (gypsum, bassanite, and anhydrite) with Fe-sulfates (jarosite) detected in relatively low abundances in some locations [5]. Some rocks also show evidence for Ca-sulfate cement, with potential Mg-sulfate cemented layers in one ~10 m interval [6].

All of the sedimentary rocks examined by CheMin contain an X-ray amorphous component (AmC), and most AmCs include some X-ray amorphous sulfur [7]. For some of these samples, SO_2 release temperatures and peak shapes from evolved gas analyses (EGA) using the SAM instrument suggest the presence of poorly crystalline or amorphous Fe- and Mg-sulfates [e.g., 8]. These materials are hypothesized to represent: amorphous sulfates, adsorbed sulfate anions, S-bearing phase inclusions in minerals or glass, oxidation of sulfides, or crystalline sulfur phases present below CheMin detection limits [8]. Here for the first time, we examine and compare the abundances and compositions of the amorphous sulfur in Gale crater rocks in order to better constrain these materials.

Methods: Bulk AmC compositions are estimated through a mass balance calculation that combines bulk sample geochemistry (APXS) with XRD-derived minerals and abundances (CheMin). Calculations were performed for all rock samples through Vera Rubin ridge (VRR; up to sol 2300) [7]. Since APXS frequently acquires multiple compositions of drill samples (e.g., undisturbed rock, drill tailings, discard pile), we used the same APXS measurements used in previous calculations, where applicable. Mineral abundances and compositions are from [9-10].

Caveats: (1) compositions of crystalline phases below the detection limit of XRD are allocated to the AmC composition; (2) minor elemental substitutions in crystalline minerals are also allocated to the AmC composition; (3) when present, poorly constrained clay mineral compositions make it difficult to precisely determine the AmC composition; for samples with ~25 wt% phyllosilicates in the crystalline component, different clay compositions result in differences of ≤ ~2 wt% CaO, MgO, and FeO_T in the AmCs [11].

Results: On average, AmCs contain ~10 wt% SO_3 (standard deviation = 5 wt%; range: ~0 - 22 wt%), and the bulk rock samples (AmC + crystalline minerals) contain on average ~4 wt% amorphous SO_3 (standard deviation = 2.6 wt%; range: ~0 - 10 wt%). Thus, between 20 and 90% of any sample's sulfur content is in the X-ray amorphous state.

AmC SO_3 contents show no strong correlation with either of the two most abundant oxides in the AmCs, SiO_2 and FeO_T (Fig. 1). Additionally, there is no systematic change in AmC SO_3 content with stratigraphic position as was observed for AmC SiO_2

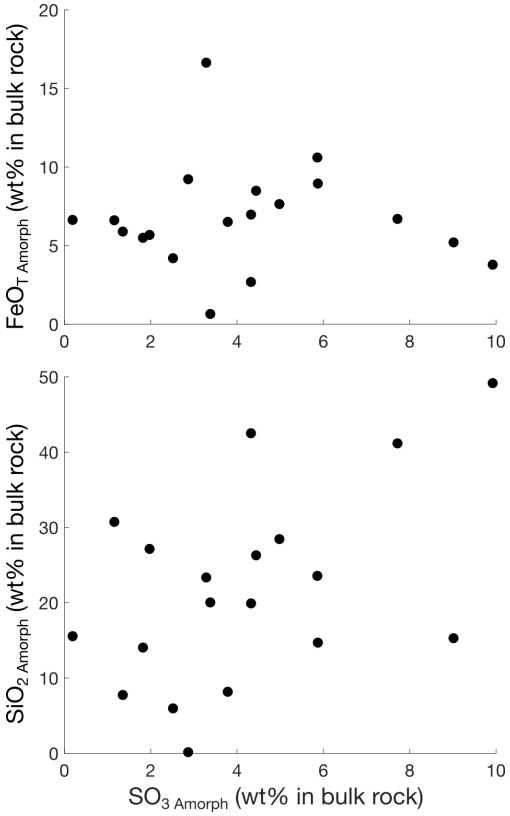

***Figure 1**. Amorphous SO_3 in bulk rock (wt%) compared to amorphous FeO_T (top) and SiO_2 (bottom) in bulk rock.*

contents [7]. Furthermore, AmC SO_3 content is not correlated with sedimentary rock lithology (e.g., sandstone vs. mudstone).

A SO_3-MgO-CaO ternary diagram (Fig. 2a) helps characterize potential compositions of the amorphous sulfur-bearing material in each drill hole location. Most of the AmCs plot over a range consistent with complex/variable mixtures of amorphous and poorly crystalline Ca-, Mg-, and Fe-sulfates with Mg- and Ca-bearing phases (e.g., silicates).

The Al_2O_3-SO_3-SiO_2 ternary diagram (Fig. 2b) illustrates that most AmCs are enriched in SO_3 and/or SiO_2 compared to Martian basalts, and some locations contain essentially no Al_2O_3 in the amorphous component (JK, CB, BK, LB, and GH). Notable is the sample WJ, which has the most SO_3-rich AmC.

Discussion: The presence of X-ray amorphous Fe-, Ca-, and Mg-sulfates is consistent with interpretations of poorly crystalline or amorphous Fe- and/or Mg-sulfates in some samples (CB, GH, and MJ) based on SAM EGA analyses; Ca-sulfates are not detectable by SAM [e.g., 8].

Based on analyses of the other major constituents of the AmCs (SiO_2 and FeO_T), it is likely that multiple processes formed the amorphous materials in Gale crater, and so there is no reason that AmC SO_3 has to correlate with other AmC constituents (i.e., indicating co-deposition). Additionally, sulfate minerals are highly soluble, and any initial correlation could have been overprinted during one of the many hypothesized late diagenetic events in Gale crater.

Since most of the crystalline Ca-sulfate detections along the traverse have been associated with observable diagenetic features that crosscut the bedrock [e.g., 2], it is reasonable to conclude that the amorphous sulfates predate the Ca-sulfate features, and could contribute to sediment cementation.

One explanation for the presence of amorphous sulfates is that initially crystalline hydrated sulfates became structurally destabilized once exposed to the temperatures and relative humidity of the modern Martian surface and/or inside the instruments [6]. For example, the dehydration of epsomite under current Mars conditions has been shown to form a hydrated amorphous Mg-sulfate [12]. Alternatively, amorphous sulfate nanoparticles have been shown to be precursors to crystalline sulfates [13].

Preliminary Conclusions: Preliminary data analysis suggests the presence of amorphous or poorly crystalline Fe-, Ca-, and Mg-sulfates. It is likely that these amorphous materials (whether precipitated as amorphous or structurally destabilized later) predate the Ca-sulfates associated with diagenetic features, and could be helping cement the sediments. Future measurements will determine if the amorphous Mg- and Fe-sulfate contents increase as we approach and then enter the upcoming mostly Mg-sulfate unit [14], or if those materials are more crystalline.

Acknowledgments: The authors are indebted to the MSL science, engineering, and management teams for their efforts in tactical and strategic operations.

References: [1] Milliken R. E. et al. (2010) *Geophys. Res. Lett.*, 37. [2] Nachon M. et al. (2014) *JGR*, 119, 1991-2016. [3] Nachon M. et al. (2017) *Icarus*, 281, 121-136. [4] Kronyak R. E. et al. (2019) *JGR*, 124, 2613-2634. [5] Rampe E. B. et al. (2020) *Geochem*., 80. [6] Rapin W. et al. (2019) *Nat. Geo*., 12, 889-895. [7] Smith R. J. et al. (2020) *LPSC LI*, Abstract #2708. [8] Sutter B. et al. (2017) *JGR*, 122, 2574-2609. [9] Morrison S. M. et al. (2018) *Am. Min*., 103(6), 857-871. [10] Achilles C. N. (2020) *JGR, 125*. [11] Dehouck E. et al. (2014) *JGR*, 119, 2640-2657. [12] Chipera S. J. and Vaniman D. T. (2007) *Geo. et Cosmo. Acta*, 71, 241-250. [13] Jia C. et al. (2020) *Cryst. Eng. Comm*., 22, 6805-6810. [14] Powell, K. E., et al. (2019) *9th Int. Conf. on Mars*, Abstract #2089. [15] Lodders, K. (1998) *Meteorit. Planet. Sci*., 33(S4), A183-A190.

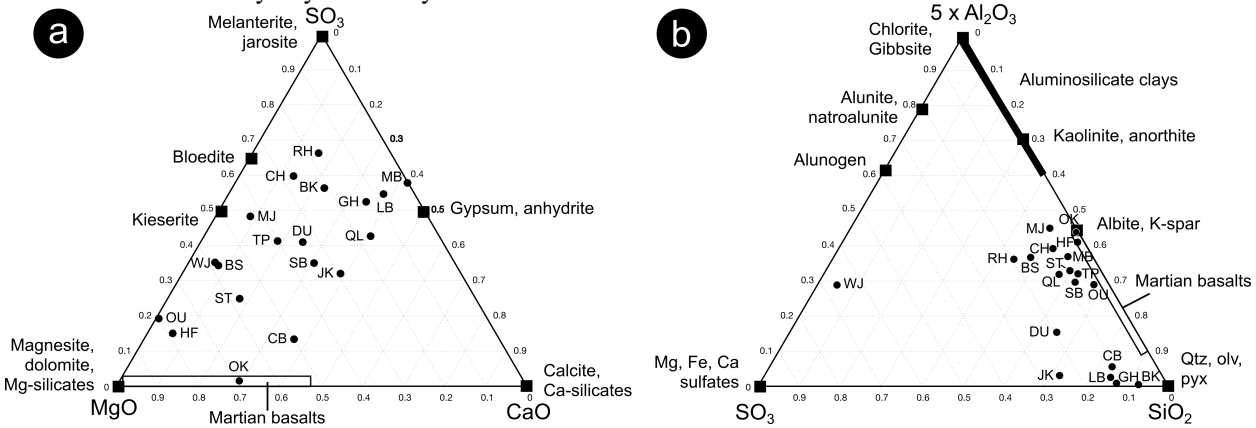

Figure 2*. Ternary diagrams comparing bulk amorphous compositions for each drill hole location, shown as black dots labeled with sample name (see below for abbreviations), to crystalline phases shown in black squares and rectangles and Martian basalts [15]. (a) Plot of mole proportions of SO_3-MgO-CaO. (b) Plot of mole proportions of (5x)Al_2O_3-(1x)SO_3-(1x)SiO_2. Drill holes: JK–John Klein, CB–Cumberland, WJ–Windjana, CH–Confidence Hills, MJ–Mojave2, TP–Telegraph Peak, BK–Buckskin, OU–Oudam, MB–Marimba, QL–Quela, SB–Sebina, DU–Duluth, ST–Stoer, HF–Highfield, RH–Rockhall, BS–Big Sky, OK–Okoruso, GH–Greenhorn, LB–Lubango.*